

# Development of the Sealed-Type Triple-Point-of-Argon Cell for Long-Stem SPRT Calibration at KRISS

I. Yang · C. H. Song · K. H. Kang · Y. -G. Kim ·  
K. S. Gam

Published online: 23 April 2008  
© Springer Science+Business Media, LLC 2008

**Abstract** A system was fabricated to realize the triple point of argon for the calibration of long-stem standard platinum resistance thermometers. A cryostat was constructed so that the temperature could be controlled quasi-adiabatically, and the melting was realized using the continuous-heating method. The combined uncertainty of the realization of the triple point of argon for a confidence level of 95% was 0.6 mK.

**Keywords** Calibration · Long-stem SPRT · Triple point of argon · Thermometry

## 1 Introduction

Long-stem standard platinum resistance thermometers (SPRTs) can be used for temperatures as low as the triple point of argon (83.8058 K) [1] and, therefore, they must be calibrated directly at the triple point of argon, or by comparison with a previously calibrated capsule-type SPRT [2]. The design of an apparatus for the cryogenic fixed-point calibration of long-stem SPRTs must take into account the fact that the available depth is limited by the distance between the sensing element and the head of the SPRT. Thus, a temperature gradient of  $>200$  K occurs over a length  $<50$  cm [3–7]. Therefore, controlling the heat flow is essential to realizing the cryogenic fixed point when calibrating long-stem SPRTs. In this work, a sealed triple-point-of-argon cell for calibrating long-stem SPRTs was constructed, and its realization uncertainty is presented.

---

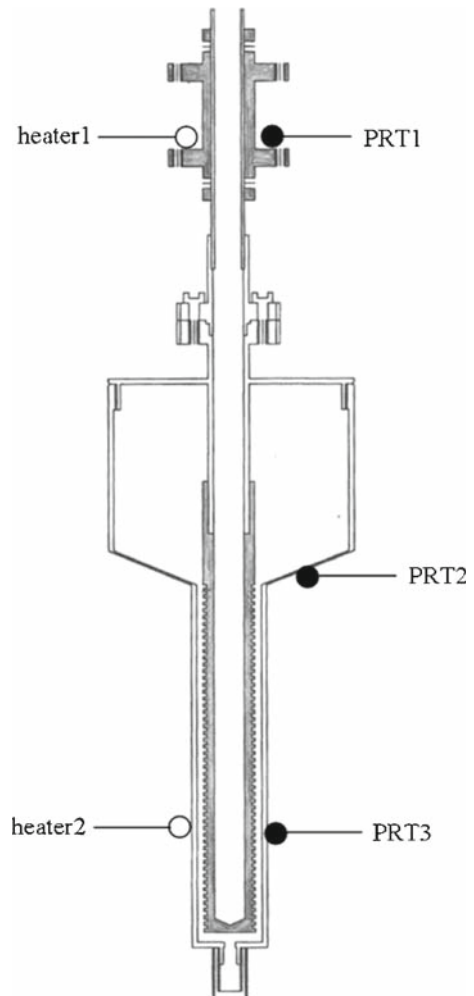
I. Yang (✉) · C. H. Song · K. H. Kang · Y.-G. Kim · K. S. Gam  
Division of Physical Metrology, Korea Research Institute of Standards and Science (KRISS),  
1 Doryong-dong, Yuseong-gu, Daejeon, 305-340, South Korea  
e-mail: iyang@kriss.re.kr

## 2 Argon Cell and the Cryostat

### 2.1 Design of the Argon Cell

Figure 1 shows a schematic diagram of the sealed argon cell. The cell was designed so that a long-stem SPRT with a diameter up to 7.5 mm could be inserted for calibration. The cell is made of stainless steel, except for the lower part of the thermometer well, which is made of copper. The inner volume of the cell to be filled with the thermometric gas was calculated to be  $234\text{ cm}^3$ . In our design, if the cell is filled with argon gas at a pressure of 60 atm (6.1 MPa) at room temperature, then a depth of about 10 cm of solid argon will be formed at temperatures below the triple point of argon. After

**Fig. 1** Design of the triple-point-of-argon cell used to calibrate the long-stem SPRTs. The shaded parts are made of copper, whereas all the other parts are made of stainless steel. Dimensions are indicated in Fig. 2



filling the cell with argon gas at a pressure of 60 atm, the cell was cut from the argon charging system using a pinch-sealing method.

The temperature of the copper plate located approximately 70 mm from the top of the cell is monitored using an uncalibrated industrial platinum resistance thermometer (PRT) designated PRT1. Two other PRTs, designated PRT2 and PRT3—as shown in Fig. 1, monitor the temperature at two different positions on the cell. Heaters are installed on both the copper plate and the cell to control the temperature and to induce the melting of argon.

## 2.2 Thermometric Gas

High-purity argon gas purchased from Messer (Germany) was used in this work. According to the certificate provided by the manufacturer, the impurities in the gas are less than 1.7 volume parts per million (vppm). The dominant impurities are oxygen, nitrogen, and water, which are claimed to be present at concentrations <0.5 vppm each.

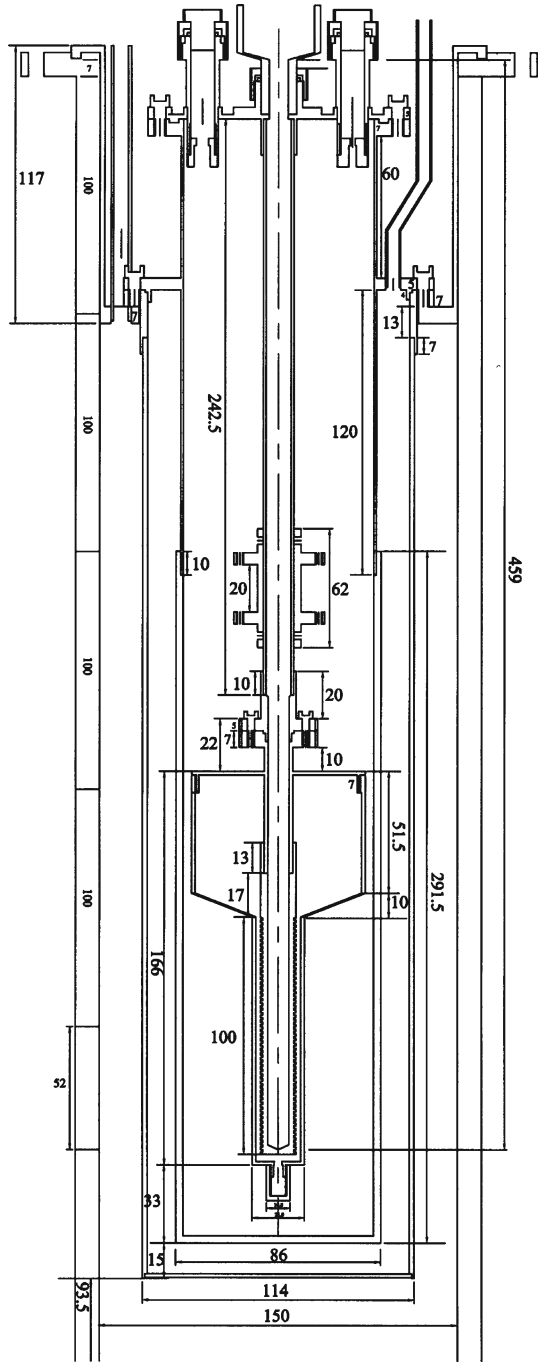
## 2.3 Cryostat

Figure 2 shows the cryostat used to realize the triple point of argon and designed to calibrate long-stem SPRTs whose stems are longer than 400 mm. The dimensions shown in Fig. 2 are in millimeters. Most of the parts are made of stainless steel, with the exception of some parts where high thermal conductivity is essential. The argon cell attaches to the SPRT well guide, which is made of stainless steel. An indium seal is used to seal the inner chamber so that a high vacuum (approximately  $10^{-7}$  torr) can be maintained during the realization of the triple point. The lower half of the inner chamber, up to the height corresponding to the top of the argon cell, is made of copper. Electrical wires for the measurements are heat-sunk to a temperature near that of liquid nitrogen and connected to the vacuum feedthrough on top of the chamber. The inner chamber is placed in a Dewar filled with liquid nitrogen during the realization of the triple point of argon.

## 2.4 Measurement Equipment

The long-stem SPRT used in this work was a Rosemount (USA) 162CE S/N 4931. The resistance ratio of this thermometer with respect to a standard resistor (Tinsley, UK, Model 5685A, nominal resistance = 25  $\Omega$ ) was measured using an Automatic Systems Laboratories (ASL, UK) Model F900 AC resistance bridge. The carrier current was 1 mA, at a frequency of 30 Hz. The gain of the bridge during the realization of the triple point was  $10^5$ , and data readings were taken every 30 s. The resistances of PRT1 and PRT3 were monitored using a digital multimeter in the four-wire resistance mode. To characterize the quality of the realization of the triple point of argon, PRT2 was monitored using a device with a higher resolution than that used for PRT1 or PRT3, either

**Fig. 2** Schematic diagram of the cryostat and the cell for the realization of the triple point of argon. Dimensions shown are in mm



an ASL F700 or an ASL F18 resistance bridge, depending on the required resolution of the measurement.

### 3 Results and Uncertainty

#### 3.1 Realization of the Triple Point

The cryostat was cooled from room temperature by filling the Dewar with liquid nitrogen, and charging the cryostat with a pressure of a few tens of torr of helium exchange gas. This procedure took about 90 min to reach a temperature below the triple point of argon, starting from room temperature. To realize the triple point, the temperature of the copper plate was controlled to a temperature 0.17 K above the temperature of the triple point of argon. To achieve this, a heating power of 3.4 mW was applied to the copper plate using heater 1. Figure 3 shows the resistance ratio of the SPRT in two representative realizations of the triple point of argon. Five melting plateaux were used to evaluate the average bridge reading and its repeatability. The duration of the melting of the argon depended on the temperature of the copper plate (measured using PRT1) and on how well the temperature could be controlled. For some SPRTs, the heat flow from the stem of the SPRT was too high. Therefore, it was difficult to control the temperature of the copper plate below a given temperature, and the temperature at the copper plate was too high. For thermometers with a small heat flow through the stem, the commercial temperature controller with a proportional–integral–differential control program could maintain the temperature at the copper plate within  $\pm 10$  mK. When the temperature of the copper plate was well controlled, the melting of the

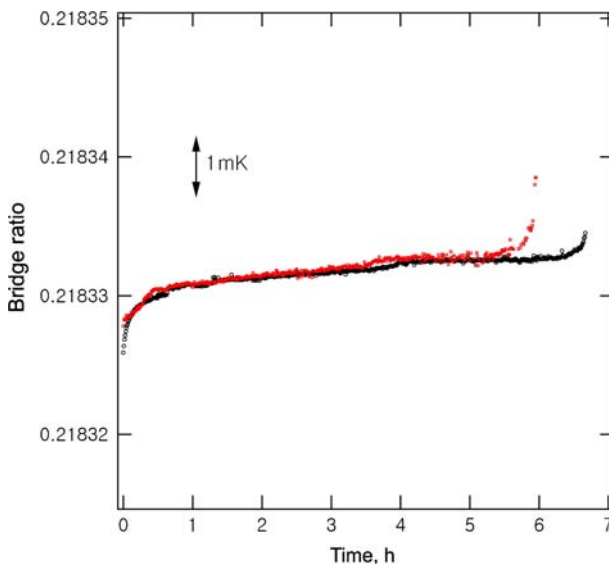


**Fig. 3** Two representative plateaux selected from five melting points of argon that were used to evaluate the value of  $W$  and to determine its repeatability

argon took more than 6 h, and the temperature rise over a period of 4 h in the middle of the melting period was  $<0.35$  mK. The average bridge reading was determined from the five melting plateaux weighted by the duration of the plateau, i.e., the number of available data points in a fixed data acquisition interval of 30 s.

## 3.2 Uncertainty

### 3.2.1 Determination of the Plateau Value

The uncertainty resulting from the choice of the plateau value was determined from the melting data sets shown in Fig. 3. The uncertainty was taken as the maximum deviation of the bridge reading, after eliminating the first and final 10% of the balanced signal. We note that this is a rather conservative way of determining the uncertainty of the melting plateau value. The standard uncertainty determined from this melting set was 0.16 mK, assuming a rectangular distribution.

### 3.2.2 Plateau Repeatability

The repeatability of the plateau was taken to be the standard deviation of the average bridge readings from five realizations of the melting point of argon. The standard deviation was equivalent to 0.10 mK with the  $t$ -distribution, and the number of degrees of freedom was  $\nu = 4$ .

### 3.2.3 Chemical Impurities

From the gas manufacturer's certificate, the impurity content of the argon gas was less than 1.7 vppm. Using the overall maximum estimate methodology [8] with the first cryoscopic constant of argon, the uncertainty due to the chemical impurities was 0.048 mK. Assuming that the relative uncertainty of the impurity analysis is 100% of the declared uncertainty of the manufacturer, then the degree of freedom of this uncertainty component is  $\nu = 2.6$  [8].

### 3.2.4 Self-Heating

The effect of self-heating on the SPRT model used in this work for a current of 1 mA was  $<0.1$  mK when a " $\sqrt{2}$  test" was performed during the triple-point plateau. We treated this increase itself as the uncertainty from the self-heating, and this component was equated to a rectangular distribution with a standard deviation of 0.03 mK.

### 3.2.5 Heat Flux

The influence of the external heat flux was estimated from the temperature variation around the cell measured using PRT2 and PRT3, as shown in Fig. 4. Note that the digital multimeter used to measure the output from PRT3 had a much lower resolution

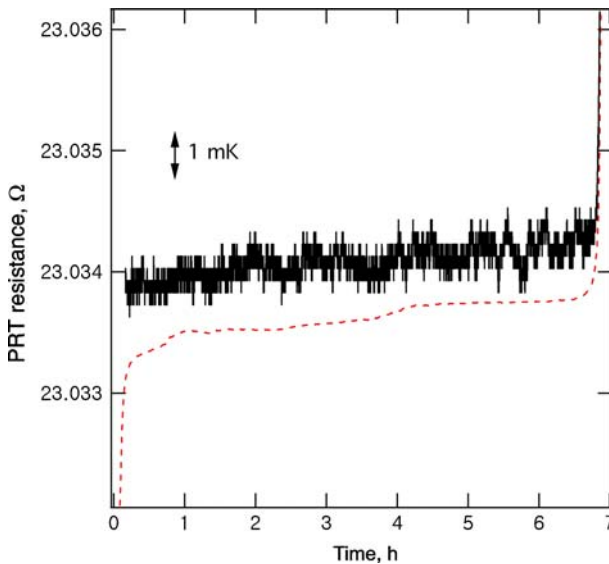


**Fig. 4** Resistances of PRT2 (dashed line) and PRT3 (solid line) during the melting plateau of argon

and sensitivity than the AC bridge used to measure the output from PRT2, and therefore the noise from PRT3 was not from the actual temperature variation. Furthermore, since the two PRTs were *not* calibrated, the difference between the resistances of the two PRTs has no physical significance. The variation in each PRT reflects the change in temperature occurring during the melting plateau. From the variation in the temperature indicated by the two PRTs attached to the outer surface of the cell, we estimated that the standard uncertainty resulting from the external heat flux was 0.15 mK.

### 3.2.6 Standard Resistors

The calibration certificate obtained from the electrical group at KRISS stated that the  $k = 1$  uncertainty of our standard resistor was 0.25 ppm. Assuming that the temperature variation of the resistor bath was less than 0.1 K, and the temperature coefficient of the resistor was consistent with the product's specification ( $2 \text{ ppm} \cdot \text{K}^{-1}$ ), then the standard uncertainty of the standard resistor was 0.54 ppm. This corresponds to an uncertainty of 0.02 mK in determining the triple point of argon.

### 3.2.7 Hydrostatic Head Correction

The depth of the solid–liquid surface in our sealed cell was 100 mm. Since the sensing part of the SPRT used in our work was 50 mm in length, the effective depth below the liquid surface was 75 mm. Therefore, the hydrostatic head correction was 0.248 mK. Although we used this value to correct for the hydrostatic head effect, we also took this value as the full width of a rectangular distribution in determining the uncertainty

**Table 1** Uncertainty budget for the calibration of long-stem SPRTs at the triple point of argon

Uncertainty component	Standard uncertainty (mK)	Degrees of freedom
Determination of the plateau value	0.160	$\infty$
Plateau repeatability	0.110	4
Chemical impurity	0.048	2.6
Self-heating <sup>a</sup>	0.030	$\infty$
Heat flux	0.150	$\infty$
Standard resistor	0.020	$\infty$
Hydrostatic head correction	0.072	$\infty$
Propagation from TPW uncertainty	0.022	$\infty$
Expanded uncertainty $U_{95}$	0.6	–

<sup>a</sup> Only applicable to the particular model of SPRT used in this work

as we do not have any immersion profile data at this point. Therefore, the standard uncertainty component from the hydrostatic head correction was 0.072 mK.

### 3.2.8 Propagation from TPW Uncertainty

The standard uncertainty in realizing the value of the TPW in our calibration of the SPRTs at KRISS was 0.1 mK. Therefore, the uncertainty propagated from the resistance at the TPW was 0.022 mK, considering the resistance ratio,  $W$ , at the triple point of argon.

### 3.2.9 Expanded Uncertainty

Table 1 summarizes the uncertainty budget in realizing the triple point of argon for the calibration of long-stem SPRTs together with the degrees of freedom for each component. Our results indicate that the uncertainty of our sealed triple-point-of-argon system for a confidence level of 95% was  $U_{95} = 0.6$  mK.

## 4 Conclusions

A sealed argon cell cryostat for the calibration of long-stem SPRTs was constructed and tested using a continuous-heating method. The expanded uncertainty of our system for a confidence level of 95% was 0.6 mK, which is thought to be sufficient for long-stem SPRTs, as the repeatability and long-term stability of such sensors are usually comparable to or higher than this uncertainty value, according to the manufacturer's specification.

Our uncertainty evaluation indicates that the two large uncertainty components are the determination of the melting plateau value and the plateau repeatability, both of which were assessed conservatively in this work. An international comparison (APMPT-K3.a) is planned for long-stem SPRTs at the triple point of argon among national metrology institutes in the Asia-Pacific region. We are currently modifying our cryostat to improve the temperature uniformity in the cryostat during the realization of the triple point. Regardless of this improvement, a calibration service for



fixed point SPRTs up to the triple point of argon, and a calibration by comparison for temperatures down to  $-190^{\circ}\text{C}$ , has begun at KRISS.

## References

1. H. Preston-Thomas, *Metrologia* **27**, 3 (1990)
2. T.J. Quinn, *Temperature*, 2nd edn. Monographs in Physical Measurement (Academic Press, London, 1990), pp. 175–182
3. J. Ancsin, M.J. Phillips, *Metrologia* **5**, 3 (1969)
4. G.T. Furukawa, W.R. Bigge, J.L. Riddle, in *Temperature: Its Measurement and Control in Science and Industry*, vol. 4, part 1, ed. by H.H. Plumb (ISA, Pittsburgh, 1972), pp. 197–202
5. P. Bloembergen, G. Bonnier, H. Ronsin, *Metrologia* **27**, 101 (1990)
6. M.G. Ahmed, Y. Hermier, M.R. Moussa, G. Bonnier, in *Temperature: Its Measurement and Control in Science and Industry*, vol. 7, part 1, ed. by D.C. Ripple (AIP, New York, 2002), pp. 197–202
7. S.L. Pond, in *Temperature: Its Measurement and Control in Science and Industry*, vol. 7, part 1, ed. by D.C. Ripple (AIP, New York, 2002), pp. 203–208
8. *Document CCT/05-08*, “Methodologies for the estimation of uncertainties and the correction of fixed-point temperatures attributable to the influence of chemical impurities,” Consultative Committee for Temperature